Efficacy of atmospheric pressure dielectric barrier discharge for inactivating airborne pathogens

Jaione Romero-MangadoAvishek DeyDiana C. Diaz-Cartagena, Nadja E. Solis-Marcano, Marjorie López-Nieves, and Vilynette Santiago-GarcíaDennis NordlundSatheesh KrishnamurthyM. Meyyappan and Jessica E. KoehneRam P. Gandhiraman

Citation: Journal of Vacuum Science & Technology A: Vacuum, Surfaces, and Films **35**, 041101 (2017); doi: 10.1116/1.4990654

View online: http://dx.doi.org/10.1116/1.4990654

View Table of Contents: http://avs.scitation.org/toc/jva/35/4

Published by the American Vacuum Society

Efficacy of atmospheric pressure dielectric barrier discharge for inactivating airborne pathogens

Jaione Romero-Mangado
Science and Technology Corporation, Moffett Field, California 94035

Avishek Dey
Universities Space Research Association, Mountain View, California 94043 and Materials Engineering, The Open University, Milton Keynes MK7 6AA, United Kingdom

Diana C. Diaz-Cartagena, Nadja E. Solis-Marcano, Marjorie López-Nieves, and Vilynette Santiago-García
Department of Chemistry, University of Puerto Rico, Río Piedras Campus, San Juan 00931, Puerto Rico

Dennis Nordlund
Stanford Synchrotron Radiation Lightsource, SLAC National Accelerator Laboratory, Menlo Park, California 94025

Satheesh Krishnamurthy
Materials Engineering, The Open University, Milton Keynes MK7 6AA, United Kingdom

M. Meyyappan and Jessica E. Koehne
NASA Ames Research Center, Moffett Field, California 94035

Ram P. Gandhiraman[a)]
Universities Space Research Association, Mountain View, California 94043

(Received 25 March 2017; accepted 16 June 2017; published 5 July 2017)

Atmospheric pressure plasmas have gained attention in recent years for several environmental applications. This technology could potentially be used to deactivate airborne microorganisms, surface-bound microorganisms, and biofilms. In this work, the authors explore the efficacy of the atmospheric pressure dielectric barrier discharge (DBD) to inactivate airborne *Staphylococcus epidermidis* and *Aspergillus niger* that are opportunistic pathogens associated with nosocomial infections. This technology uses air as the source of gas and does not require any process gas such as helium, argon, nitrogen, or hydrogen. The effect of DBD was studied on aerosolized *S. epidermidis* and aerosolized *A. niger* spores via scanning electron microscopy (SEM). The morphology observed on the SEM micrographs showed deformations in the cellular structure of both microorganisms. Cell structure damage upon interaction with the DBD suggests leakage of vital cellular materials, which is a key mechanism for microbial inactivation. The chemical structure of the cell surface of *S. epidermidis* was also analyzed by near edge x-ray absorption fine structure spectroscopy before and after DBD exposure. Results from surface analysis revealed that reactive oxygen species from the DBD discharge contributed to alterations on the chemistry of the cell membrane/cell wall of *S. epidermidis*. © *2017 American Vacuum Society*.
[http://dx.doi.org/10.1116/1.4990654]

I. INTRODUCTION

Staphylococcus epidermidis is a Gram-positive bacterium that colonizes the human epithelium. *S. epidermidis* emerges as an opportunistic pathogen and a common cause for nosocomial infections leading to chronic infections.[1–3] These microorganisms have the ability to form biofilms on medical implants and catheters.[4–6] This bacterium is a coagulase-negative *Staphylococcus* that causes infection in immune-compromised, long-term hospitalized and critically ill patients.[7,8] Low temperature plasmas offer an efficient and robust approach for the sterilization of surfaces, medical devices, surgical tools, material processing, and microelectronics.[9–11] The efficiency of different types of plasmas such as plasma from plasma torch or vacuum based plasmas differ according to the nature of plasma generation, gas mixtures, flow rates, temperature, and treatment area.[12,13] The aim of this study is to investigate the efficacy of an atmospheric pressure dielectric barrier discharge (DBD) technology for deactivating airborne microorganisms. We studied the effects of the atmospheric pressure plasma on two different types of microorganisms, Gram-positive bacteria, and fungal spores. Previous work using the DBD system was focused on *Escherichia coli*, a Gram-negative bacteria.[14] The distinctive difference between Gram-negative and Gram-positive bacteria is the presence of a thick peptidoglycan outer layer on Gram-positive bacteria whereas Gram-negative bacteria have a thin peptidoglycan structure. The mentioned study concluded that *E. coli* cell structure was damaged to varying extent and a severe oxidation of the cell membrane was found, establishing effective inactivation of the bacteria.[14]

[a)]Electronic mail: rgandhiraman@usra.edu

Spores are reproductive units able to survive in extreme conditions, resisting chemical and physical attack until the environment is favorable for growth. Airborne fungal spores can cause allergies as well as serious hospital-acquired infections. *Aspergillus niger* is a well studied fungi that causes problems related to food industry and medicine, which makes it a suitable candidate for this study.[15]

Over the past decade, there has been a growing interest in the sterilization effect of atmospheric pressure and low-pressure helium/argon/oxygen plasmas on surface-bound bacteria and spores.[16–18] The effect of atmospheric pressure plasma using process gas such as helium or argon on surface-bound *S. epidermidis* has already been studied.[19] However, there is no work on air based DBD that is low cost and does not require additional process gas. Hence, the present study is focused on the systematic effect of air based DBD (with no additional gas supply) on airborne bacteria and fungus.

This study provides a detailed morphological and spectroscopic analysis of the impact of DBD on aerosolized *S. epidermidis* and *A. niger*. DBD for airborne microbial inactivation is a radically new approach in exploring the use of atmospheric pressure plasmas by eliminating any process gas requirement and developing a process that can run continuously without any interference.

II. EXPERIMENTAL WORK

A. Materials

The chemicals used in this study were purchased from ATCC [*S. epidermidis* ATCC 14990, *A. niger* ATCC 15475 and phosphate buffered saline (PBS) ATCC SCRR-2201], Becton Dickinson (nutrient broth BD 213000, nutrient agar BD 234000 and potato dextrose agar 213400), Sigma-Aldrich (ethyl alcohol 459844, glutaraldehyde G5882, and hexamethyldisilazane 440191), and Ted Pella Inc. (osmium tetroxide 18466).

B. Culture conditions

Cultures of *S. epidermidis* were grown in nutrient broth at 37 °C, 200 rpm until the cultures reached a midlog phase. After incubation, 100 μl of the bacterial suspension was used for plating on nutrient agar after suitable dilutions. The colony forming units were counted after 16 h of incubation. Aliquots of the midlog phase cultures were then centrifuged at 1000 rpm for 10 min. The supernatant was discarded, and the cells were resuspended in distilled water.

A. niger was inoculated in sterile distilled water and incubated overnight at room temperature for propagation. *A. niger* spores were harvested aseptically in potato dextrose agar and incubated for 5 days at 24 °C. Individual spores were then isolated to conduct DBD studies.

C. Experimental setup

A compressor nebulizer was used to aerosolize bacterial cultures and spores into the DBD system (NV200, Novaerus, Inc.) for sterilization testing. The DBD system consisted of two coaxial cylindrical coils made of stainless steel (AISI: 304) wires of 0.2 mm diameter. The coils were separated by a borosilicate glass tube acting as the dielectric barrier. The glass tube is 80 mm long with an internal diameter of 22.5 mm and an outer diameter of 28 mm. The spores and bacteria were nebulized using an OMROM compressor nebulizer model NE-C29-E, and the entire setup was kept inside a biosafety cabinet (Nuaire, Class II, Type A2, Model NU-425-400). A high alternating voltage (4 kV) was applied between the electrodes to create the plasma discharge. The DBD system was equipped with a fan to draw the aerosolized output of the nebulizer. All the DBD system vents except the top one were sealed to prevent any undesired micro-organism from getting into the system.

The samples containing *S. epidermidis* and distilled water (1 ml) were transferred to the compressor nebulizer. The aerosolized bacterial suspension was then passed through the discharge via the top input, and any viable particles after DBD treatment were collected at the output on sterile silicon wafers (Fig. 1). Concomitantly, the fungal suspension containing *A. niger* spores and distilled water (1 ml) was transferred to the compressor nebulizer and recirculated through the DBD system. Any viable spores were collected at the output of the system on previously sterilized silicon wafers (Fig. 1).

D. Characterization

To image the bacterial cells and fungal spores using scanning electron microscopy (SEM), the cells were fixed on a silicon wafer using the following process. The protocol included fixing in a solution of 2.5% glutaraldehyde in PBS for 2 h. To improve the contrast during SEM imaging, the samples were postfixed in a 2% osmium tetroxide in PBS for 1.5 h. The samples were then dehydrated in graded concentrations of ethanol (60%–100%) for 50 min and finally chemically dried with hexamethyldisilazane for 5 min. The samples were placed in a vacuum desiccator overnight to prevent reactions with water and humidity. The fixation of fungal spores was carried out in the same way.

SEM imaging was performed using a S4800 scanning electron microscope (Hitachi, Pleasanton, CA) with single

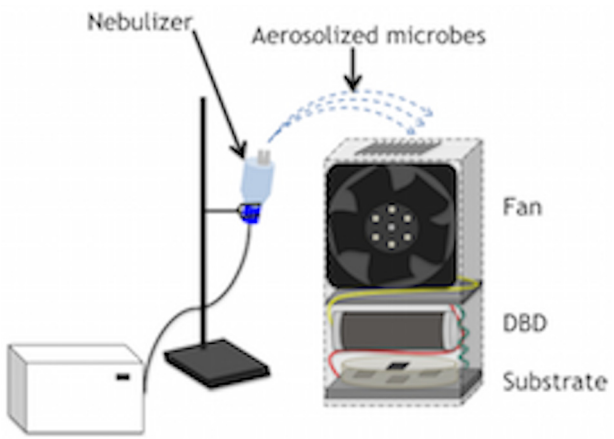

FIG. 1. (Color online) Schematic of the experimental setup.

side polished silicon wafers as substrates. All the samples were coated with a 10 nm layer of gold to negate the charging effect.

To understand the possible mechanism for deactivation of cells, we used x-ray absorption spectroscopy. This spectroscopic technique provides a range of x-ray energies that are applicable to most elements in the periodic table suitable for determining the changes in surface chemistry of bacteria. Near edge x-ray absorption fine spectroscopy (NEXAFS) measurements were carried out at beamline 8–2 (bending magnet end station, spherical grating monochromator) at Stanford Synchrotron Radiation Lightsource.[20] The incoming flux was monitored using a gold grid placed in the beam path upstream of the chamber. The samples were mounted on an aluminum stick and placed on a load lock before transferring for analysis at an ultrahigh vacuum chamber ($<1 \times 10^{-9}$ mbar). The chamber is equipped with a PHI 15–255 G double pass cylindrical mirror analyzer that was used for total electron yield collection through the sample-drain current. All the measurements were carried out at the incident magic angle of ~55° (magic angle). NEXAFS spectra were normalized 20–30 eV above the ionization potential after dividing by the incoming flux measured at the gold grid. X-ray absorption spectroscopy (XAS) data were analyzed using the IGOR PRO software following standard normalization protocols, including incoming flux normalization, linear background removal, and atomic normalization (high energy normalization). For these measurements, the bacterial samples collected on silicon wafers were freeze-dried using a Labconco's Free Zone 4.5 l Freeze Dry System.

III. RESULTS AND DISCUSSION

A. Morphological studies of the microorganisms

S. epidermidis samples were drop-casted on silicon wafer, fixed using standard protocols and imaged under SEM. These images reveal the size, shape, and morphology of the bacteria. From the SEM images (Fig. 2), it is evident that the *S. epidermidis* has dimensions of less than 1 μm. The plasma inactivation experiment can be seen as having three groups of variables, one being the nebulization, one being the fan that pulls the air toward the discharge and the other the electrodes that create the discharge. As a control experiment, nebulized *S. epidermidis* was passed through the DBD system with both the fan and DBD turned off. To isolate the effect of the fan, another control experiment was performed in which the DBD was turned off while the fan was on. Figure 2 shows the SEM images of *S. epidermidis* at different settings before DBD treatment. The observed structures are spherical bacteria, with dimensions of less than 1 μm and without visible changes in the morphology.

To study the effect of DBD on the microbes, the microorganisms were passed through the system with both the fan and DBD turned on. Figures 3(a)–3(c) show that *S. epidermidis* has lost its spherical shape and texture, and the cell structure is severely damaged resulting in complete distortion. It is apparent from the SEM images that the bacteria underwent severe structural damage to varying

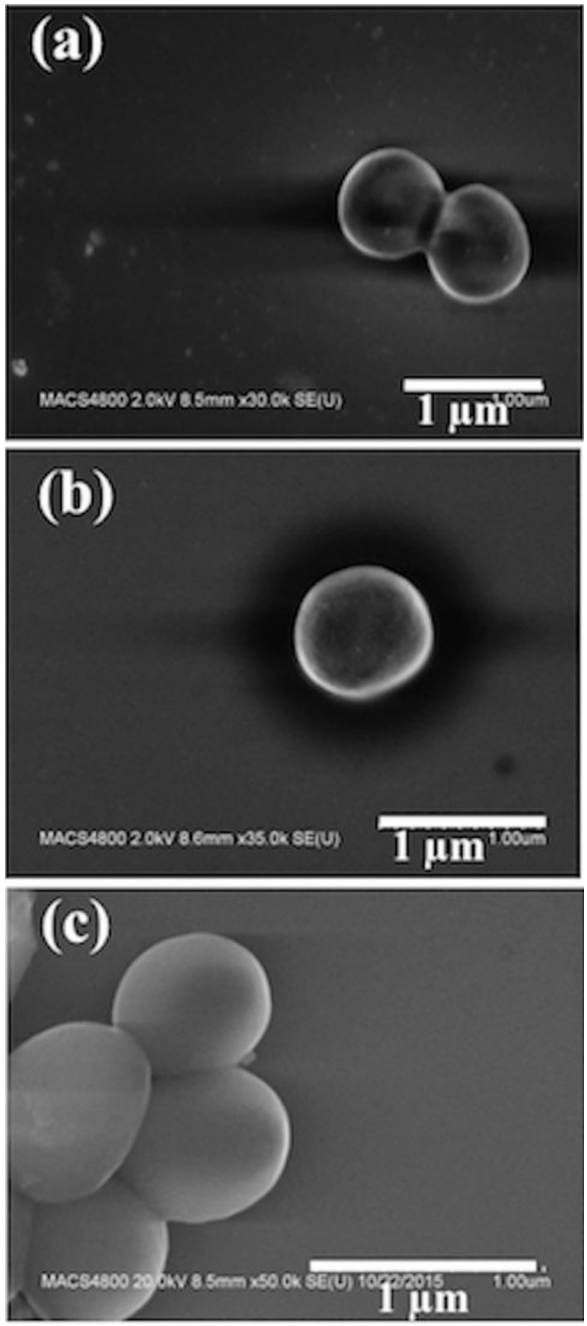

FIG. 2. SEM images of (a) drop casted *S. epidermidis* on silicon wafer, (b) aerosolized and collected in a silicon wafer with both DBD and Fan OFF, (c) aerosolized and collected in a silicon wafer with just Fan ON.

degrees, resulting in breakage of cell structure, although not all microbes undergo structural damage to the same extent.

Chitosan, a polysaccharide known for its antifungal activity, causes molecular disorganization and structural alterations of the cytoplasm and plasma membrane.[21,22] Plascencia-Jatomea *et al.* studied the effect of chitosan and temperature on *A. niger* and reported morphological changes of the spores upon treatment with chitosan.[23] To demonstrate the effectiveness of our approach, spores of *A. niger* were supplied through the DBD system. The fungal spores, which are hard to annihilate were completely deformed after

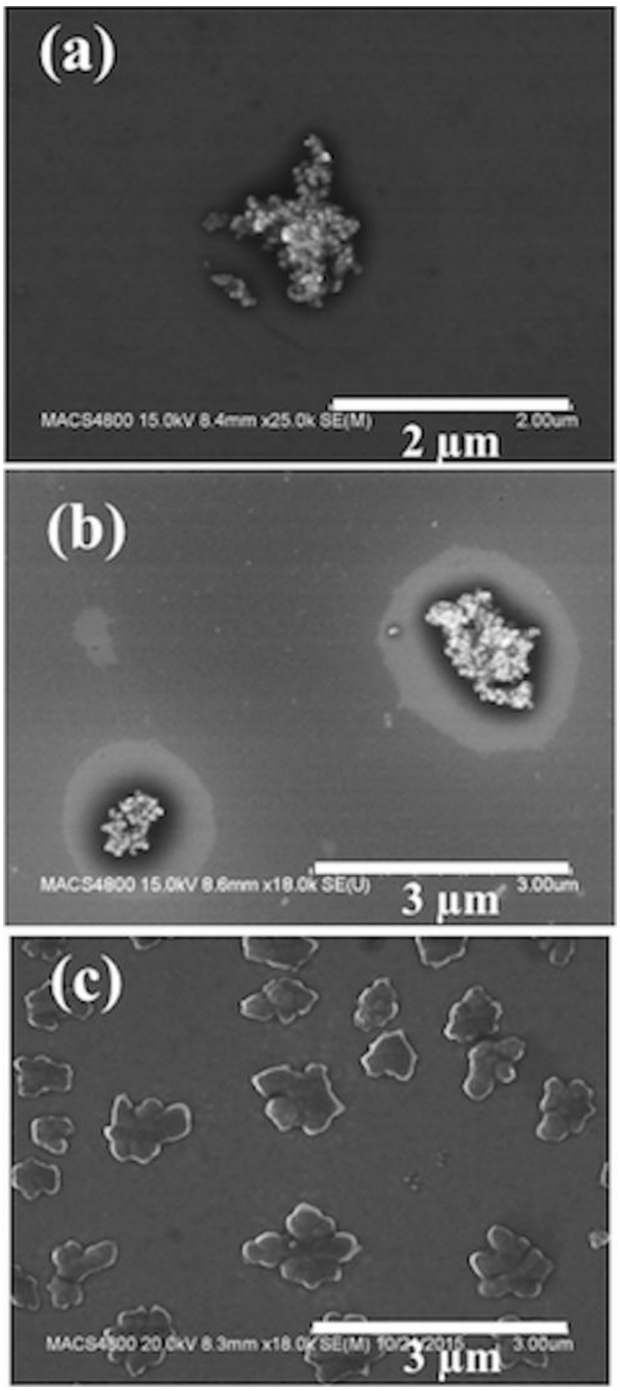

FIG. 3. (a)–(c) High resolution SEM images of *S. epidermidis* after passing through the DBD discharge showing severe deformation of the cell structure to varying degrees.

passing through the plasma discharge. Figures 4(a)–4(c) show spherical and clumped spores before exposure to the plasma discharge.[23] Figure 4(b) shows asexually produced fungal spores formed on a conidiophore in a 2 μm scale.

After passing through the discharge, the round shaped fungal spores are found to be completely disfigured as shown in Figs. 4(d)–4(f). The morphological anomalies are evident in the fungal spores treated with DBD. High resolution images [Figs. 4(e) and 4(f)] of the treated fungus confirm that the cell envelope integrity is broken upon DBD treatment. Reduction in size and severe distortion of the DBD treated spores indicate possible structural damage of the cell resulting in breakage of spores. It is evident from Fig. 4(d) that the spores were echinulate. A similar observation was made by Plascencia-Jatomea *et al.*, in their work on chitosan based antifungal activity and attributed the echinulate spore formation to chitosan affected swelling.[23]

B. Surface chemical analysis

In order to understand the influence of plasma on surface chemistry, NEXAFS studies were carried out only on the *S. epidermidis* samples. NEXAFS spectra from each functionalized state at the carbon K edge, nitrogen K edge, and oxygen K edge (absorption edges) are shown in Fig. 5. NEXAFS is highly surface sensitive and changes in partial density of states will reveal the influence of nearest neighbor and highlight the effect of DBD on the bacteria surface. Figure 5(a) demonstrates the comparison between the surface functionalization states of control with DBD off (F) and on (N) conditions. As the fan has no effect on the bacteria morphology, the fan was kept on for both the cases just to identify the changes in surface chemistry of the bacteria due to DBD. The peak at 285.5 eV in the carbon spectra [Fig. 5(a)] of all the samples correspond to π^* C=C transitions.[24] The intensity drop at 285.0 eV may be due to the effect of normalization of the spectra as it matches with the carbon dip from the beamline optics. The shoulder at 286.7 eV corresponds to π^* (C−OH) and π^* (C−O−C) transitions, which gets prominent after plasma treatment. The control sample shows negligible presence of aliphatic carbon species (C–H, 287.8 eV). For N instead, there is significant presence of aliphatic carbon at the surface. The increase in intensity of peak 287.8 eV can be related to the breaking of C=C bonds to form C−OH, aliphatic C−H and C−O−C species at the surface.

In Fig. 5(a), the intense peak at 288.5 eV for the untreated bacteria arises from the π^* (C=O) transitions and might be from either −COOH or $-CONH_2$ moieties. Previous studies on inner shell excitation spectroscopy of the peptide bonds and proteins revealed that the π^* (C=O) transitions occurs between 288.2 and 288.6 eV.[25] A shift of 0.4 eV is observed for N at π^* (C=O) transitions relative to the control sample. This red shift has been attributed to the increase in electronegativity of the carbonyl core induced by the neighboring atoms as reported by Urquhart and Ade from OH to nitrogen containing groups.[26] Edwards and Myneni also reported the same in their NEXAFS studies of bacterial hydroxamate sidephores in aqueous solutions.[27] The peak at 289.4 eV for the control sample could be due to various functional groups, since C–H and O-alkyl C groups in polysaccharides/carboxylic acids or CNHσ^* all have transitions at this energy value.[25,28] The broad peak in the region of 292–295 eV for all the samples comprises of multiple σ^* transitions, e.g., C–N in amino acids (291 eV)[29] and C–O in alcohols and carboxylic acids (292.5 eV).[30,31] A small peak at 297.5 eV is likely due to σ^*C−OH transitions which is less prominent for the DBD on state. The broad peak around 304.0 eV for

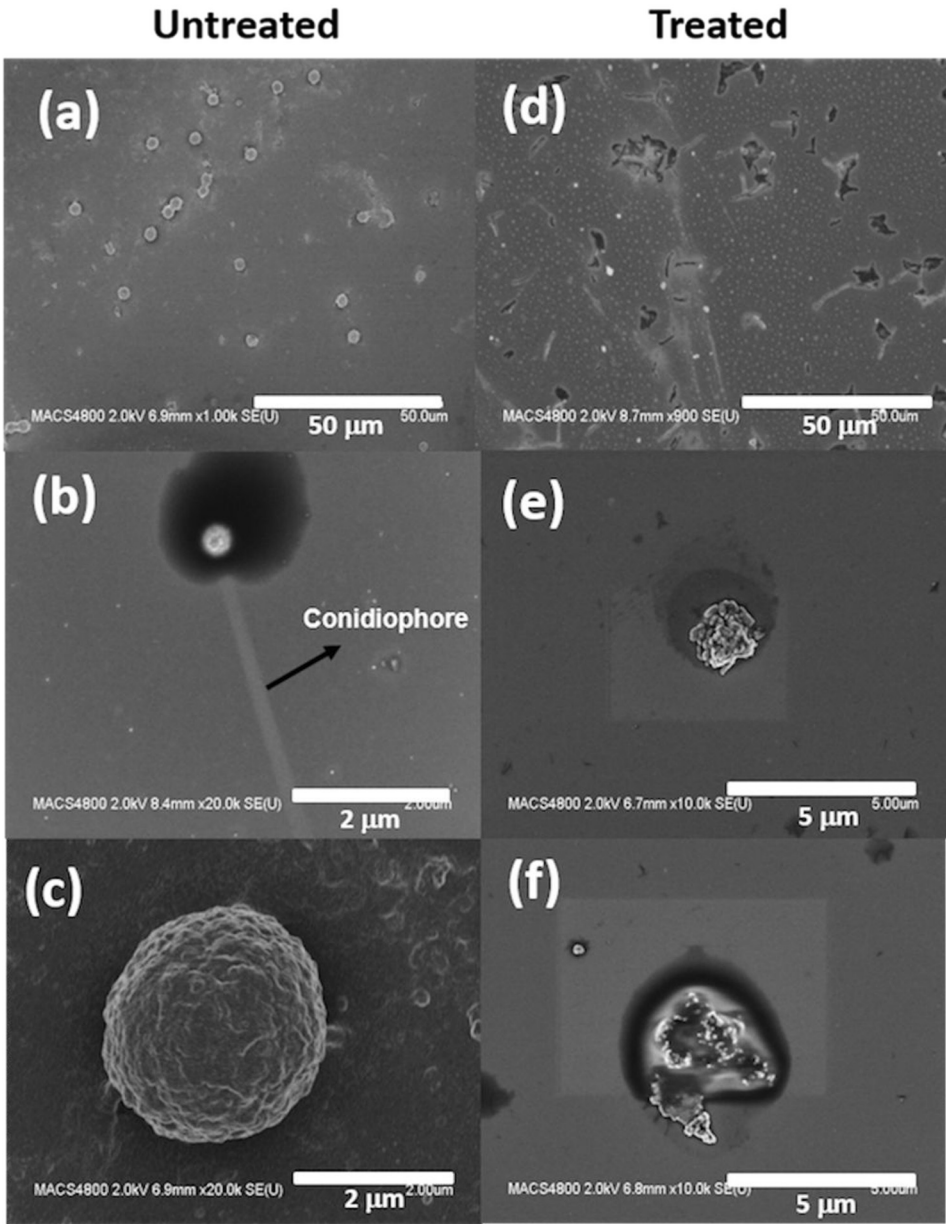

FIG. 4. (a) Low resolution SEM images of *A. niger* spores before passing through the discharge, showing spherical shape of the fungus. (b) and (c) High resolution images of *A. niger* before passing through the discharge showing intact cell structure. (d) Low resolution SEM images of *A. niger* after passing through the discharge showing echinulate formation. (e) and (f) High resolution SEM images of *A. niger* after passing through the discharge showing severe distortion and destruction of the cell structure.

untreated bacteria corresponds to σ^*C=C transitions. The spectral signature of various carbon moieties varied at different areas of the substrate for N. The uniformity of plasma functionalization also depends on the extent of exposure. When the fan is on, the duration of interaction of the bacteria with plasma is not uniform compared to the fan off condition. In the fan off state, the bacteria have an extended interaction with the plasma, resulting in consistent spectral signature throughout the substrate.

The O K edge spectra [Fig. 5(b)] for the control sample exhibit an intense peak at 531.6 eV corresponding to π^* transitions of oxygen double bond moieties, COOH and $CONH_2$ functionalities, which is considerably smaller for all other samples (N > F).[25] Both C K edge and O K edge spectra indicate to the decreased concentration of C=O groups with respect to the control sample. The untreated sample shows a broad peak around 536–540 eV which can be due to contributions from multiple transitions comprising of Rydberg transitions, σ^*O–H and σ^*C–O transitions.[25,30,32] For samples F and N this broad peak can be clearly resolved into two peaks centered around 537 and 539 eV, that are due to alcoholic (σ^*O–H),and single bonded oxygen sigma (σ^*C–O) transitions, respectively.[14] However, it can be noticed that for N samples the (σ^*O–H) and (σ^*C–O) transition peaks are red shifted. This observation is similar to the π^* (C=O) transitions at 288.5 in C K edge.

The nitrogen K-edge [Fig. 5(c)] show a low intensity peak at 398.7 eV that corresponds to N1s to π^* (N=C)

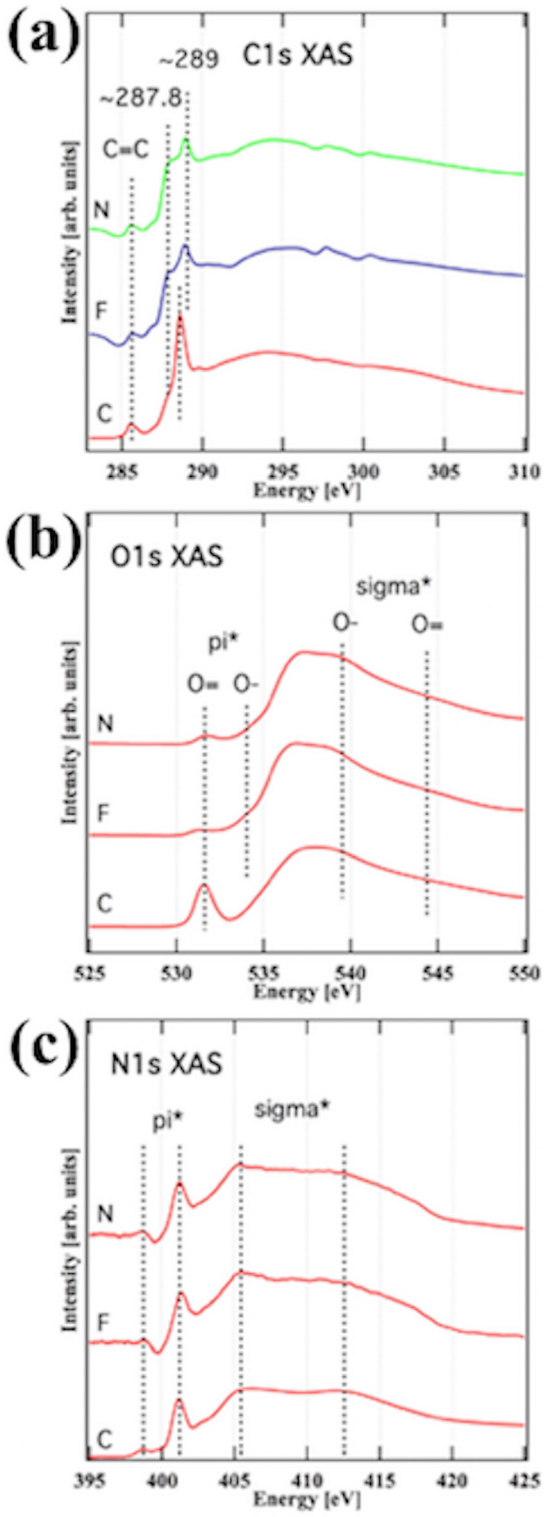

FIG. 5. (Color online) Core level near edge x-ray absorption fine spectroscopy spectra of (a) carbon K-edge, (b) oxygen K-edge, and (c) nitrogen K edge. C corresponds to control sample, F corresponds to DBD off, and N corresponds to DBD on.

transitions, and an intense peak around 401.5 eV related to the electronic transitions of amide groups [$\pi^*_{(C=O)NH}$]. The decrease in intensity of this amide peak is consistent with the reduction of carbonyl functionalities seen in C1s and O1s spectra. For the untreated sample the broad peak around 405 eV can originate from multiple transitions including σ^* N–C and Rydberg transitions.[25,33] The sharpening of this peak for F and N is likely due is likely due to the reduction of the different N-C environment, and potentially an increased concentration of nitro groups at the surface of the bacteria. The broad peak around 412.0 eV can be designated to the σ^* (N=C) transitions in accordance to the reported value of Shard *et al.*[34] For F and N, another peak can be observed around 416 eV which is absent for untreated bacteria, possibly due to σ^* (N=O) transitions. Although it is hard to deny the contribution of contaminants from the substrate and the limited spectral contrast that is observable for our low bacteria coverage on the silicon, the exposure to the plasma clearly modifies not only the morphology but also the chemical functionalities at the surface of the bacteria.

The carbon, nitrogen and oxygen bonding environments on the surface of the microbes clearly changed upon treatment with DBD. Atmospheric pressure plasmas sustained in ambient air contains short lived and highly reactive nitrogen and oxygen species like ozone, hydrogen peroxide, hydroxyl radical, and various NOx species. These active species can directly or indirectly affect the structure and function of proteins, lipids, and nucleic acids (DNA damage).[35] This is evident from increased signal intensity of single bonded oxygen bonds including OH and CO in O K edge XAS. Also a sharp rise in 405 eV peak, in N XAS, corresponding to p* transition of nitro group is a clear evidence of oxidation of the cell surface. Both the reactive nitrogen and oxygen species have been reported to cause irreversible cytoplasmic membrane damage and damage of the cell integrity eventually causing bacterial death.[36] NEXAFS for the *S. epidermidis* revealed that the deactivation resulted from damage to the chemical backbone at the surface. The changes in molecular environment of C–O, C–N, and C–C bonds are evident from the NEXAFS spectra. We attribute these changes to hydrogen bonding as can be seen from C K edge peak at 287.8 eV and the gradual disappearance of O p* from O K edge. Much work needs to be done in order to completely understand the mechanism behind these novel systems.

Overall, the data gathered from this study denotes damages and changes at the cell structure level in Gram-positive bacteria and fungal spores when treated with DBD. When cell lysis occurs, lipopolysaccharides are released eliciting immune responses such as febrile reactions in animals. Further experimentation will need to be conducted to determine the effect of the oxidized cell wall debris and other reactive species after DBD treatment. Based on the assumption that animals respond the same way that humans do when exposed to certain products, animal studies with healthy adult rabbits will be done. These studies will evaluate the health effects of pyrogens released from microbial inactivation via DBD in humans.

IV. SUMMARY AND CONCLUSIONS

We have explored the efficacy of the atmospheric pressure dielectric barrier discharge for inactivating airborne *S. epidermidis* and *A. niger* spores. A systematic study was

carried out to understand the effect of DBD on the morphology of these microorganisms. The aerosolized microbial samples were collected from air in the vicinity of the DBD and were analyzed for surface chemical and morphological changes upon DBD treatment. The SEM images showed that the targeted microorganisms underwent physical distortion to varying degrees resulting in loss of cellular materials. The DBD causes cell structure damage, leading to destruction of cellular components and resulting in cell death. The element specific NEXAFS study revealed that the changes in the surface chemistry, in particular, to the hydrogen bonding, altered the chemical environment at the surface of bacteria leading to inactivation. The changes in molecular bonding environment of carbon and oxygen were clear for the aerosolized bacteria that pass through the system with DBD on and off conditions. The C K edge of the DBD on samples, in comparison to DBD off, exhibited increased intensity of C–OH and C–O–C and a red shift of π^* (C=O) transition all arising due to increase in electronegativity of carbonyl core. Similarly in O K edge, the edges corresponding to (σ^*O–H) and (σ^*C–O) transition are red shifted for DBD on samples compared to DBD off condition. All these indicate oxidation of the surface and formation of more hydroxyl groups and carbonyl groups on the surface of DBD treated samples.

ACKNOWLEDGMENTS

Use of the Stanford Synchrotron Radiation Lightsource, SLAC National Accelerator Laboratory, was supported by the U.S. Department of Energy, Office of Science, Office of Basic EnergySciences under Contract No. DE-AC02-76SF00515. The contents of this publication are solely the responsibility of the authors and do not necessarily represent the official views of NIGMS, NIH, or NASA.

[1]W. Ziebuhr, S. Hennig, M. Eckart, H. Kränzler, C. Batzilla, and S. Kozitskaya, Int. J. Antimicrob. Agents **28**, 14 (2006).
[2]G. Y. C. Cheung, K. Rigby, R. Wang, S. Y. Queck, K. R. Braughton, A. R. Whitney, M. Teintze, F. R. DeLeo, and M. Otto, PLos Pathog. **6**, 1001133 (2010).
[3]M. Otto, Nat. Rev. Microbiol. **7**, 555 (2009).
[4]M. Otto, Curr. Top. Microbiol. **322**, 207 (2008).
[5]J. W. Costerton, P. S. Stewart, and E. P. Greenberg, Science. **284**, 1318 (1999).
[6]C. Vuong and M. Otto, Microbes Infect. **4**, 481 (2002).
[7]P. Domingo and A. Fontanet, AIDS Patient Care STD **15**, 7 (2001).
[8]W. Ziebuhr, Contrib. Microbiol. **8**, 102 (2001).
[9]G. Fridman, G. Friedman, A. Gutsol, A. B. Shekhter, V. N. Vasilets, and A. Fridman, Plasma Process Polym. **5**, 503 (2008).
[10]G. E. Morfill, M. G. Kong, and J. L. Zimmermann, New J. Phys. **11**, 115011 (2009).
[11]M. H. Lee, B. J. Park, S. C. Jin, D. Kim, L. Han, J. Kim, S. O. Hyun, K. H. Chung, and J. C. Park, New J. Phys. **11**, 115022 (2009).
[12]K. D. Weltmann, E. Kindel, T. von Woedtke, M. Hähnel, M. Stieber, and R. Brandenburg, Pure Appl. Chem. **82**, 1223 (2010).
[13]M. G. Kong, G. Kroesen, G. Morfill, T. Nosenko, T. Shimizu, J. van Dijk, and J. L. Zimmermann, New J. Phys. **11**, 115012 (2009).
[14]J. Romero-Mangado *et al*., Biointerphases **11**, 11009 (2016).
[15]E. Schuster, N. Dunn-Colleman, J. C. Frisvad, and P. W. M. van Dijck, Appl. Microbiol. Biotechnol. **59**, 426 (2002).
[16]M. Laroussi, Plasma Process Polym. **2**, 391 (2005).
[17]G. Daeschlein, T. von Woedtke, E. Kindel, R. Brandenburg, K. D. Weltmann, and M. Jünger, Plasma Process. Polym. **7**, 224 (2010).
[18]M. Laroussi, IEEE Trans. Plasma Sci. **37**, 714 (2009).
[19]R. Matthes, I. Koban, C. Bender, K. Masur, E. Kindel, K.-D. Weltmann, T. Kocher, A. Kramer, and N.-O. Hübner, Plasma Processes Polym. **10**, 161 (2013).
[20]K. G. Tirsell and V. P. Karpenko, Nucl. Instrum. Methods A **291**, 511 (1990).
[21]D. Zhang and P. C. Quantick, J. Hortic. Sci. Biotechnol. **73**, 763 (1998).
[22]S. Roller and N. Covill, Int. J. Food Microbiol. **47**, 67 (1999).
[23]M. Plascencia-Jatomea, G. Viniegra, R. Olayo, M. M. Castillo-Ortega, and K. Shirai, Macromol. Biosci. **3**, 582 (2003).
[24]S. Sainio, D. Nordlund, R. Gandhiraman, H. Jiang, J. Koehne, J. Koskinen, M. Meyyappan, and T. Laurila, J. Phys. Chem. C **120**, 22655 (2016).
[25]M. L. Gordon, G. Cooper, C. Morin, T. Araki, C. C. Turci, K. Kaznatcheev, and A. P. Hitchcock, J. Phys. Chem. A **107**, 6144 (2003).
[26]S. G. Urquhart and H. Ade, J. Phys. Chem. B **106**, 8531 (2002).
[27]D. C. Edwards and S. C. B. Myneni, J. Phys. Chem. A **110**, 11809 (2006).
[28]D. Solomon, J. Lehmann, J. Kinyangi, B. Liang, and T. Schafer, Soil Sci. Soc. Am. J. **69**, 107 (2005).
[29]K. Kaznacheyev, A. Osanna, C. Jacobsen, O. Plashkevych, O. Vahtras, H. Ågren, V. Carravetta, and A. P. Hitchcock, J. Phys. Chem. A **106**, 3153 (2002).
[30]D. A. Outka, J. Stöhr, R. J. Madix, H. H. Rotermund, B. Hermsmeier, and J. Solomon, Surf. Sci. **185**, 53 (1987).
[31]F. Sette, J. Stoühr, and A. P. Hitchcock, J. Chem. Phys. **81**, 4906 (1984).
[32]J. Stewart-Ornstein, A. P. Hitchcock, D. Hernández Cruz, P. Henklein, J. Overhage, K. Hilpert, J. D. Hale, and R. E. W. Hancock, J. Phys. Chem. B **111**, 7691 (2007).
[33]A. Vairavamurthy and S. Wang, Environ. Sci. Technol. **36**, 3050 (2002).
[34]A. G. Shard, J. D. Whittle, A. J. Beck, P. N. Brookes, N. A. Bullett, R. A. Talib, A. Mistry, D. Barton, and S. L. McArthur, J. Phys. Chem. B **108**, 12472 (2004).
[35]A. Privat-Maldonado, D. O'Connell, E. Welch, R. Vann, and M. W. van der Woude, Sci. Rep. **6**, 35646 (2016).
[36]L. Han, S. Patil, D. Boehm, V. Milosavljević, P. J. Cullen, and P. Bourke, Appl. Environ. Microbiol. **82**, 450 (2016).